



Evaluation of NiWO_4 as an oxygen carrier for the hydrogen storage by chemical looping.

P.E. González-Vargas; M.J. Meléndez-Zaragoza; J.M. Salinas-Gutiérrez; V. Collins-Martínez; A. López-Ortiz*

Centro de Investigación en Materiales Avanzados, S.C., Miguel de Cervantes 120, Complejo Industrial Chihuahua
Chihuahua, Chih. México. C.P. 31136

* Tel: +52 6144394815; e-mail: alejandro.lopez@cimav.edu.mx

ABSTRACT

Chemical looping process (CL) have recently been used for various purposes, one of which is the hydrogen storage using metal oxides (MeO) as the only source of oxygen (oxygen carriers) to produce water ($\text{MeO} + \text{H}_2 = \text{Me} + \text{H}_2\text{O}$) and regenerating the metal oxide with a steam oxidizing atmosphere for the hydrogen release ($\text{Me} + \text{H}_2\text{O} = \text{MeO} + \text{H}_2$). It is important that these oxygen carriers have certain characteristics to be used for this purpose, such as thermal stability and the ability to store and release the lattice oxygen to the cyclic reaction conditions. In order to evaluate the nickel tungstate (NiWO_4) for this purpose, it was thermogravimetrically tested (TGA) in three accelerated redox cycles using a mixture of 5 v% of H_2/Ar as a reducing atmosphere and a mixture of 5 v% $\text{H}_2\text{O}/\text{Ar}$ gas stream as the oxidizing atmosphere. Characterization made to the material before and after the redox cycles were performed by XRD, BET surface area, and SEM and have shown its favorable potential as an oxygen carrier when testing its thermal and reactive stability after three consecutive redox cycles. TGA tests revealed an oxidation mechanism of the reduced metals (Ni + W) that follows a reaction path, which consists in the formation of WO_3 by the oxidation of W with steam, followed by the formation of NiWO_4 . This reaction path was confirmed by thermodynamic calculations that indicate that the oxidation of Ni, WO_3 and steam is presumably the rate-determining step.

Keywords: NiWO_4 ; redox reaction; chemical hydrogen storage; chemical looping.

1. Introduction

Although it is difficult to determine energy consumption in a precise way in the future, it is a fact that it will increase significantly in the coming decades. This is mainly due to the constant growth of the human population, which in turn demands the consumption of diverse natural

September 18th to 21st, 2018 in Mexico City, Mexico.



XVIII International Congress of the Mexican Hydrogen Society

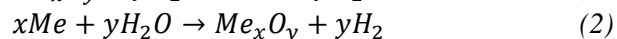
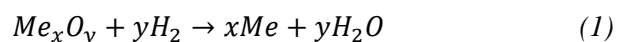


resources to satisfy basic needs. Such is the case of the use of fossil fuels, mainly used to obtain electricity, transport and for artificial air conditioning of buildings. It is due to the decrease of these fuels and the environmental impacts that they generate that a large number of researchers around the world find themselves searching for alternative energy sources and sustainable raw materials [1].

In recent times, hydrogen (H_2) has been of great interest, since it is considered as raw material for a wide variety of processes. For example, with nitrogen in the synthesis of ammonia, with CO and CO_2 to produce methanol, in the manufacture of medicines, production of hydrogen peroxide, in the electronics and petrochemical industries and to produce numerous chemical products in various syntheses [1-3]. Moreover, hydrogen is considered a clean source of energy because it has been reported to be a key element in the generation of clean and sustainable energy systems. Virtually any source of fuel, whether renewable or non-renewable, containing in its molecular structure hydrogen atoms (H) can be used for the generation of hydrogen as a gas (H_2). Due to its high energy efficiency (122 kJ/g), hydrogen has great potential to reduce dependence on oil and reduce GHG emissions, with an energy yield 2.75 times higher than that of hydrocarbons. Currently, hydrogen production accounts for around 2% of primary energy demand [4].

Nowadays, various physical and chemical methods for hydrogen storage have been proposed. Such as high-pressure and cryogenic-liquid storage, adsorptive storage on high-surface-area adsorbents, chemical storage in metal hydrides and complex hydrides, storage in boranes, carbon materials, and metal organic frameworks [5, 6]. However, each storage method has its advantages and difficulties due to safety, size, weight, cost and efficiency requirements [7].

To overcome the difficulties presented by many methods of hydrogen storage, recently, the use of redox reactions with metal oxides (MeO) under a chemical looping (CL) reaction scheme has been proposed. This principle of hydrogen storage is based on reactions (1) and (2) [5].



In order to be used in CL process, MeO species must be thermally stable to withstand the temperature gradients which are subjected during the process, to be able to store and release lattice oxygen at reaction conditions, and have good availability and affordable costs [8]. The most common MeO reported is iron oxide in its different oxidation states (Fe_3O_4 , Fe_2O_3) and this process is commonly known as the steam-iron process. This process consists in the reduction of the iron oxide with H_2 for the H_2 storage, and the subsequent liberation of the H_2 when oxidizing the Fe with steam [9-11]. The theoretical maximum storage capacity of H_2 in this process is 4.8 wt% of Fe [5], i.e., based on the Fe as the only reactive solid. However, most of the processes suggested in various research works propose the impregnation and/or support on different materials of the iron oxide to improve the storage capacity and to avoid the material sintering [5, 9, 11-14], which causes generation of an additional inert load to the reactors, which in turn causes the reduction of up to 3 times the storage capacity of H_2 based on the total solids in the reactive species (including Fe).

In other studies related to the chemical looping partial oxidation of methane (CLPO), it has been reported that some mixed metal oxides used as oxygen carriers (OC), such as perovskites

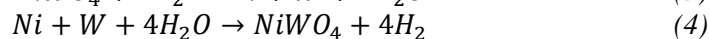
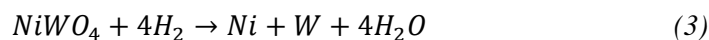
September 18th to 21st, 2018 in Mexico City, Mexico.



and ilmenites (ABO_3), are resistant to high temperatures [15, 16]. These investigations attribute the thermal resistance of the material to the cation A, while high valence B cations would contribute to the catalytic action. An example of these materials is ilmenite ($FeTiO_3$) that is reported by Schwebel et al. [17] as an OC for H_2 , CO and CH_4 as reducing gases, finding kinetics similar to previously reported, with the exception of the reaction with CH_4 , which was lower due to limitations in the surface area. These materials are reported without the addition of inert solid species for their operation, a feature that may be of advantage in CL storage of H_2 .

The cobalt tungstate ($CoWO_4$) proposed by De Los Ríos et al. [8, 18], doped with nickel (Ni) as a catalyst, reported that is highly stable before cyclic redox tests. In subsequent work, it is reported that this same material is capable of carrying out redox cycles at temperatures below $800^\circ C$ and thermal efficiencies comparable to the literature [19]. This type of materials present a high thermal resistance, are stable to cyclic redox conditions due to the phenomenon of the solid diffusional reactive barrier [20] and theoretically, are capable of requiring lower temperatures compared to other mixed metal oxides.

Based on the principles and features of mixed metal oxides in CLPO processes, the nickel tungstate ($NiWO_4$) was selected in the present work to evaluate its thermal stability and its ability to store and release lattice oxygen through redox cycles using H_2 as the reductive and steam as oxidative atmospheres to study its performance as a H_2 storage material. The involved CL redox reactions of $NiWO_4$ with H_2 and H_2O are the following:



2. Materials and Methods

2.1 Synthesis

The $NiWO_4$ was synthesized by the precipitation method at room temperature with constant stirring, as reported by Song et al. [21]. Solutions of 100 mL 0.7 M of $Na_2WO_4 \cdot 2H_2O$ and $Ni(NO_3)_2 \cdot 6H_2O$ were mixed. Once the precipitate was obtained, it was filtered and washed repeatedly with deionized water and then dried at $100^\circ C$ for 2 hours. After dried, it was calcined at $600^\circ C$ for 5 hours and allowed to cool at room temperature.

2.2 Characterization

Characterization of the calcined sample was examined to study its crystalline structure, surface area, morphology and microanalysis composition by X-ray diffraction analysis (XRD), BET surface area, scanning electron microscopy (SEM), and energy dispersive X-ray spectroscopy (EDS), respectively.

The XRD, SEM and EDS analyzes were performed on the sample before and after three redox cycles, in order to establish the stability of the material.

2.3 TGA Evaluation of Redox Cycles

The redox behavior of the $NiWO_4$ powder was followed by a conventional thermogravimetric analysis (TGA) system. All redox experiments were carried out at atmospheric pressure, the total reactive gas flowrate was 100 mL/min and the amount of $NiWO_4$ sample was

September 18th to 21st, 2018 in Mexico City, Mexico.



26 mg. Prior to the reaction, the sample was heated up in an inert atmosphere (Ar) to the desired temperature (700°C) and then isothermally treated under reducing/oxidizing flow. Before switching from reduction to oxidation atmosphere and vice versa, the reactive gases that remained were removed by an argon flow for approximately 5 min.

For the reduction process, a flow composed of 5 v% of H₂ and 95 v% Ar was used. The duration of this step was determined in order to achieve complete reduction of NiWO₄ to Ni and W, i.e., approximately 20.9% of weight loss.

For the reoxidation of the reduced sample, a mixture of water vapor and argon was supplied by water saturation of an argon flow of 60 mL/min at room temperature. The duration of this step was determined in order to complete de reoxidation of Ni and W to NiWO₄ (until no mass change could be detected).

3. Results and Discussion

Figure 1a shows the XRD pattern of the synthesized material. The obtained crystallographic phase was indexed with the Match! Software, which is in agreement with the nickel tungstate diffractogram ICSD collection code 015852 [22].

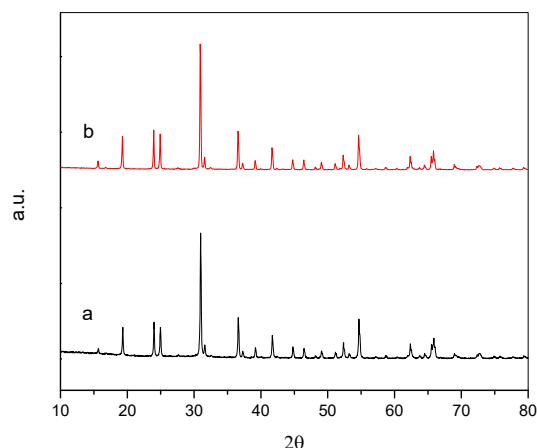


Fig. 1. X-Ray diffraction pattern of the fresh sample (a) and after the three redox cycles (b).

Figure 1b shows the XRD pattern from the sample after being exposed to three redox cycles in a TGA. The obtained crystallographic phase was indexed (as in Figure 1a) with the nickel tungstate diffractogram ICSD collection code 015852, i.e., the same crystallographic phase was present at the beginning and at the end of the redox cycles. This thermal stability can be explained based on what was reported by De Los Ríos et al. [23] that established that when the CoTiO₃ is exposed to H₂/Air redox cycles, during the reoxidation process, the cobalt returns to form the perovskite phase of titanate and cobalt, which inhibits the nucleation and migration of Co particles, thus considerably reducing the sintering process.



Table 1 shows results of BET surface area analysis and crystallite sizes of the NiWO_4 before and after of being exposed to three redox cycles. The crystallite size was determined through the characteristic signal from the samples crystalline structures and the Scherrer equation [24]:

$$\beta = \frac{0.95\lambda}{L \cos\theta}$$

Where, β is the width of the peak at half maximum intensity of a specific phase (hkl) in radians, K is a constant (0.95), λ is the wavelength of incident x-rays (0.1541 nm), θ is the center angle of the peak and finally L is the crystallite length (nm).

Table 1. BET surface area and crystallite size of the sample.

Sample	BET (m^2/g)	Fresh crystallite size (nm)	Crystallite Size – Three redox cycles (nm)
NiWO_4	4.25	47.2	56.6

According to Table 1, BET analysis results indicate a surface area within the range of other mixed metal oxides. As the mixed Fe-CeZr oxides doped with Ni reported by Sosa et al. [25] that report surface areas between 1.8 and 8.2 m^2/g .

The fresh crystallite size matches the size reported by De Los Rios et al. [20] for the CoWO_4 doped with Ni of 47.6 nm. This change in the size of the sample was expected, due to its exposure to the redox cycles at high temperatures as also reported by De Los Rios et al. [8] for the CoWO_4 after four redox cycles.

Figure 2 presents the SEM images and the EDS analysis results of the sample before and after the redox cycles. In these images, it can be observed that the fresh NiWO_4 sample is composed of sphere like particles whose sizes vary between 0.1 and 0.4 μm and forming agglomerates. In the sample after the redox cycles, it can be observed sphere like polygonal particles with an increase in particle size that ranges between 0.2 and 0.6 μm and also forming agglomerates with slight signs of sintering.

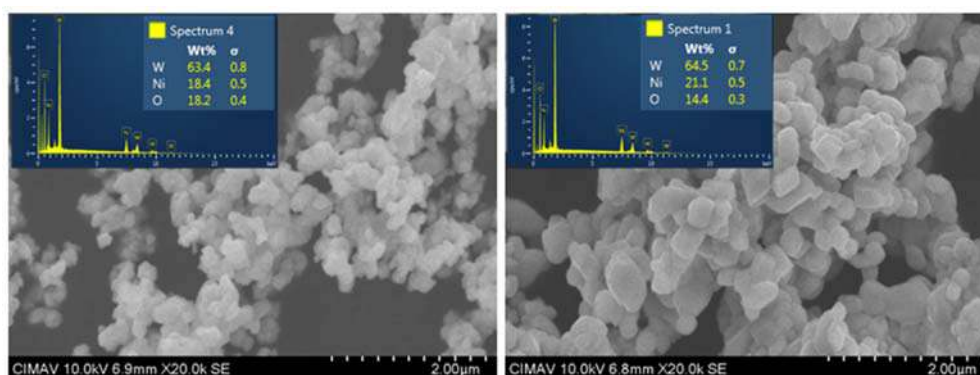


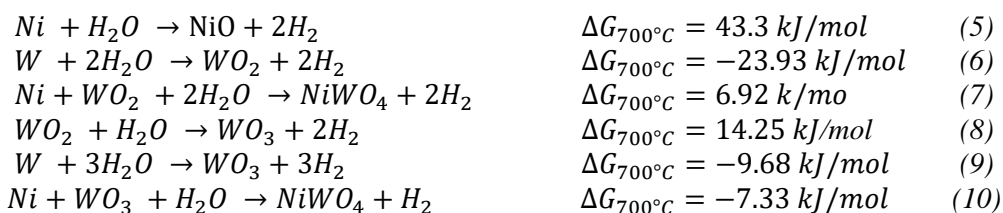
Fig. 2. SEM micrographs and EDS analysis of the fresh NiWO_4 (left) and after the redox cycles (right).



This change in morphology is due to the exposure of the material to the constant temperature of 700°C during the redox cycles. However, the signs of sintering of the material agree well with those reported by De Los Rios et al. [8], where these changes are reported to be considered not significant compared to other processes where the particle size can exceed up to one thousand times the original size after redox cycles [26]. In addition, this can be confirmed by observing that the cyclic behavior (Figure 4) and the weight composition (EDS results in Figure 3) of the material are not importantly affected within the performed cycles.

Evaluation of the storage and release of H₂ performance by TGA during three redox cycles can be observed in Figure 3. This test provides the behavior of the NiWO₄ during reduction using 5 v% H₂/Ar and reoxidation with ca. 5 v% H₂O/Ar at a constant temperature of 700°C. In this figure the weight change percentage is plotted as a function of time. The corresponding theoretical weight changes (%) from NiWO₄ (100%), the reduced metals W and Ni (79.1%), and the possible intermediate species NiO*WO₂ and Ni*WO₃ (94.8%) are represented by horizontal dotted lines. In this figure it can be observed that the material presents a high thermal stability during the redox cycles. It is also possible to observe that NiWO₄ is progressively adapting to each cycle since the reduction and oxidation times are decreasing as the number of cycles is increased. For example, in the case of the first cycle compared to the third, there is a time decrease during reduction from 85 to 60 minutes; and a decrease time during oxidation from 132 to 123 minutes. Moreover, there is a close agreement of the sample weight loss of 20.7% with respect to the theoretical value of 20.9% corresponding to the reduction of NiWO₄ to Ni and W according to reaction (3). Whereas, the experimental weight gain by oxidation was of approximately 20.7% compared to the theoretical 20.9%, corresponding to the reoxidation of Ni and W to NiWO₄ in agreement with reaction (4).

These results obtained also revealed a presumable oxidation mechanism of the reduced metals (Ni + W) that follows two oxidation stages, first W is either oxidized to WO₃ or WO₂ and secondly, Ni is oxidized by any of the previous tungsten oxide forms. The latter is because it is thermodynamically impossible to oxidize Ni with steam (see reaction 5, Gibbs free energy). Therefore, the only source of oxygen capable of regenerating the oxide must be through two reaction paths that involved the formation of WO₂ or WO₃ as intermediate species. The first path deals with the formation of WO₂ by the oxidation of W with steam and followed by the reaction of WO₂ with Ni and H₂O to form NiWO₄ according to reactions (6) and (7), respectively.



It is clear that this reaction path is not feasible, due to the fact that the reaction (7) will not thermodynamically occur because its ΔG is positive at reaction conditions (700°C). Furthermore, the formation of WO₃ from WO₂ and H₂O through reaction (8) is also not feasible ($\Delta G_{700^\circ\text{C}} = 14.25 \text{ kJ/mol}$). Therefore, the second reaction path, which consists in the formation of WO₃ by the reaction (9) followed by the formation of NiWO₄ through reaction (10) is presumably the most likely



reaction path to obtain the desired original oxide. Therefore, according to the kinetics behavior of the oxidation step it can be presumably inferred that reaction (10) should be the rate-determining step.

Furthermore, a thermodynamic equilibrium diagram shown in Figure 4 confirms that initial conditions of 1 kmol of Ni, 1 kmol of W and an excess of steam as the oxidizing atmosphere will insure the formation of NiWO_4 at equilibrium conditions.

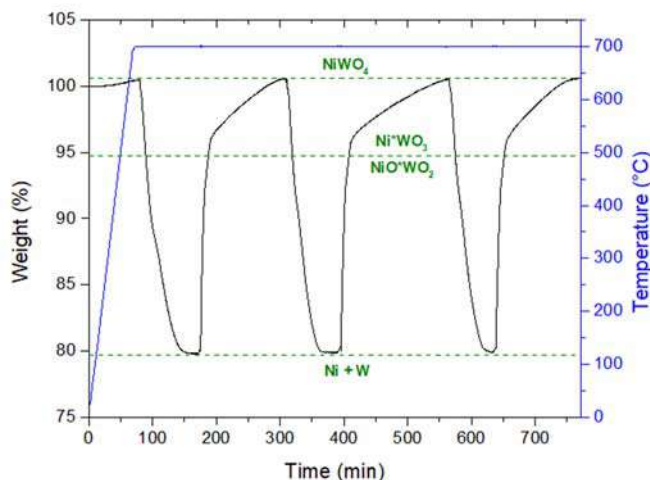


Fig. 3. TGA monitoring results of redox cycles for the sample of NiWO_4 at 700°C .

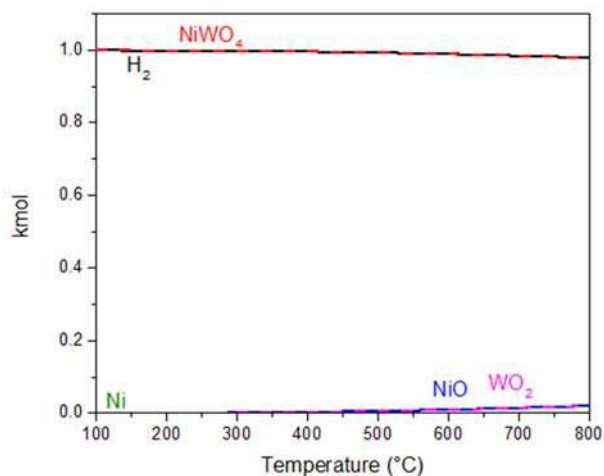


Fig. 4. Thermodynamic analysis of equilibrium composition between Ni, W, and H_2O .

A comparative H_2 storage capacity based on the total reduced solids between different previous research works can be observed in Table 2. The theoretical maximum H_2 storage capacity of NiWO_4 is 3.3 W% corresponding to a Ni/W stoichiometric ratio, which is a low capacity compared to iron oxides (4.8 W% maximum theoretical). However, it is worth to notice that this

September 18th to 21st, 2018 in Mexico City, Mexico.



proposed material is not mixed with any inert materials such as supports or dopants to improve the redox reactions and/or to prevent sintering, which makes the net loading of solids to the reactor totally reactive and the storage capacity of H₂ with respect to total solids is higher than several other Fe-based materials reported in the literature, where their capacity is reduced up to 1.4 W%.

Table 2. Comparative H₂ storage capacity of various metal oxydes.

Sample	H ₂ storage capacity based on Total solids (W%)	Reference
NiWO ₄	3.3	-
Fe ₂ O ₃ /Al ₂ O ₃ /SiO ₂	3.4	[5]
Cu-Fe/Ce/Zr	1.8	[11]
Cu/Fe/YSZ	1.8	[12]
Fe ₂ O ₃ /YSZ-GDC-Zr-Ce	1.4	[27]
Fe ₂ O ₃ /Mo/Al	4.6	[28]

4. Conclusion

Hydrogen storage and release characteristics of pure NiWO₄ using TGA redox cycles were studied. Characterization of the material (XRD, BET surface area and SEM) before and after the redox cycles shown slight signs of sintering. However, TGA evaluation indicates that these changes do not significantly affect the performance of NiWO₄ as a hydrogen storage material. The isothermal redox test yielded a hydrogen storage capacity of 3.3 wt% based on Ni/W reduced metals, which competitive with current materials reporter in the literature. Furthermore, TGA tests revealed an oxidation mechanism of the reduced metals (Ni + W) that follows a reaction path, which consists in the formation of WO₃ by the oxidation of W with steam, followed by the formation of NiWO₄. This reaction path was confirmed by thermodynamic calculations that indicate that the oxidation of Ni, WO₃ and steam is presumably the rate-determining step.

Acknowledgments

The authors of this paper wish to thank the Mexican Society of Hydrogen for accepting the proposed research for dissemination and discussion during its XVIII International Congress, as well as the scholarship. We thank equally to CONACYT for the scholarship awarded to the student involved in the project.

References

1. Sunny, A., P.A. Solomon, and K. Aparna, *Syngas production from regasified liquefied natural gas and its simulation using Aspen HYSYS*. Journal of Natural Gas Science and Engineering, 2016. **30**: p. 176-181.

September 18th to 21st, 2018 in Mexico City, Mexico.



2. De Los Ríos, T., et al., *Synthesis, characterization and stability performance of CoWO₄ as an oxygen carrier under redox cycles towards syngas production*. International Journal of Chemical Reactor Engineering, 2007. **5**(1).
3. Collins-Martinez, V., et al., *Absorption enhanced reforming of light alcohols (methanol and ethanol) for the production of hydrogen: Thermodynamic modeling*. International Journal of Hydrogen Energy, 2013. **38**(28): p. 12539-12553.
4. da Silva Veras, T., et al., *Hydrogen: Trends, production and characterization of the main process worldwide*. International Journal of Hydrogen Energy, 2017. **42**(4): p. 2018-2033.
5. Zhong, M., X. Rui, and Z. Huiyan, *Montmorillonite-Supported Iron Oxide for Hydrogen Storage by Chemical Looping*. Energy Technology, 2017. **5**(8): p. 1399-1406.
6. Eberle, U., M. Felderhoff, and F. Schueth, *Chemical and physical solutions for hydrogen storage*. Angewandte Chemie International Edition, 2009. **48**(36): p. 6608-6630.
7. Niaz, S., T. Manzoor, and A.H. Pandith, *Hydrogen storage: Materials, methods and perspectives*. Renewable and Sustainable Energy Reviews, 2015. **50**: p. 457-469.
8. De los Ríos Castillo, T., *Óxidos Metálicos Mixtos como Portadores de Oxígeno para Procesos REDOX a partir de Metano* in *Química de Materiales*. 2010, CIMAV: Chihuahua, México. p. 19, 21, 71, 121.
9. Hacker, V., R. Vallant, and M. Thaler, *Thermogravimetric investigations of modified iron ore pellets for hydrogen storage and purification: the first charge and discharge cycle*. Industrial & engineering chemistry research, 2007. **46**(26): p. 8993-8999.
10. Hui, W., S. Takenaka, and K. Otsuka, *Hydrogen storage properties of modified fumed-Fe-dust generated from a revolving furnace at a steel industry*. International journal of hydrogen energy, 2006. **31**(12): p. 1732-1746.
11. Kim, H.-S., et al., *Chemical hydrogen storage and release properties using redox reaction over the Cu-added Fe/Ce/Zr mixed oxide medium*. Journal of Industrial and Engineering Chemistry, 2010. **16**(1): p. 81-86.
12. Kim, H.-S., et al., *Hydrogen storage and release properties of a Cu-added Fe/YSZ redox system*. Journal of Nanomaterials, 2013. **2013**: p. 8.
13. Kim, Y.H., et al. *Hydrogen storage and release by redox reaction of iron oxide medium with Mo and Zr additives*. in *Advanced Materials Research*. 2012. Trans Tech Publ.
14. Kim, Y.H., et al. *Effect of Mo and Ce additives on redox behavior for hydrogen storage and release of iron oxide mediums*. in *Advanced Materials Research*. 2012. Trans Tech Publ.
15. Mihai, O., D. Chen, and A. Holmen, *Catalytic consequence of oxygen of lanthanum ferrite perovskite in chemical looping reforming of methane*. Industrial & Engineering Chemistry Research, 2010. **50**(5): p. 2613-2621.
16. Rydén, M., et al., *Combined oxides as oxygen-carrier material for chemical-looping with oxygen uncoupling*. Applied Energy, 2014. **113**: p. 1924-1932.
17. Schwebel, G.L., et al., *Apparent kinetics derived from fluidized bed experiments for Norwegian ilmenite as oxygen carrier*. Journal of Environmental Chemical Engineering, 2014. **2**(2): p. 1131-1141.
18. De los Ríos Castillo, T., et al., *Global kinetic evaluation during the reduction of CoWO₄ with methane for the production of hydrogen*. International Journal of Hydrogen Energy, 2013. **38**(28): p. 12519-12526.

September 18th to 21st, 2018 in Mexico City, Mexico.



XVIII International Congress of the Mexican Hydrogen Society



19. López-Ortiz, A., et al., *Thermodynamic analysis and process simulation of syngas production from methane using CoWO 4 as oxygen carrier*. International Journal of Hydrogen Energy, 2017.
20. De Los Ríos-Castillo, T., et al., *Study of CoWO4 as an Oxygen Carrier for the Production of Hydrogen from Methane*. Journal of New Materials for Electrochemical Systems, 2009. **12**(1): p. 55-61.
21. Song, Z., et al., *Synthesis of NiWO4 nano-particles in low-temperature molten salt medium*. Ceramics International, 2009. **35**(7): p. 2675-2678.
22. Match!®, *Calculated from ICSD using POWD-12++* 1997. p. 238
23. De los Rios, T., et al., *Redox Stabilization Effect of TiO2 in Co3O4 as Oxygen Carrier for the Production of Hydrogen through POX and Chemical Looping Processes*, in *International Journal of Chemical Reactor Engineering*. 2005.
24. Patterson, A., *The Scherrer formula for X-ray particle size determination*. Physical review, 1939. **56**(10): p. 978.
25. Vázquez, M.S., et al., *Synthesis gas production through redox cycles of bimetallic oxides and methane*. Journal of New Materials for Electrochemical Systems, 2009. **12**: p. 029-034.
26. S., T., S. V., and O. K., *Stotage and supply of pure Hydrogen from methane mediated by modified Iron Oxides* Energy & Fuels, 2004. **18**: p. 820-829.
27. Kosaka, F., et al., *Iron oxide redox reaction with oxide ion conducting supports for hydrogen production and storage systems*. Chemical Engineering Science, 2015. **123**: p. 380-387.
28. Hui, W., et al., *Hydrogen production by redox of bimetal cation-modified iron oxide*. international journal of hydrogen energy, 2008. **33**(23): p. 7122-7128.

September 18th to 21st, 2018 in Mexico City, Mexico.